JOURNAL OF MATERIALS SCIENCE 30 (1995) 4032–4036

Study of valence states of copper in copper–phosphate glasses

G. D. KHATTAK*, M. A. SALIM, A. B. HALLAK‡, M. A. DAOUS‡, E. E. KHAWAJA‡
Department of Physics, and ‡Energy Research Laboratory (Research Institute), King Fahd University of Petroleum and Minerals, Dhahran 31261, Saudi Arabia

L. E. WENGER, D. J. THOMPSON
Department of Physics, Wayne State University, Detroit, MI 48202, USA

Phosphate glasses containing CuO with composition, $[(CuO)_x(P_2O_5)_{1-x}]$, $x=0.10$, 0.20, 0.25, 0.30, 0.40 and 0.50, were studied by magnetization, X-ray photoelectron spectroscopy (XPS) and Rutherford backscattering spectrometry (RBS). It was observed that compositional changes take place in going from batch to glass and these changes are more pronounced for low copper concentration. The ratio $[Cu^{2+}/Cu_{total}]$ as a function of x was determined from XPS and magnetization combined with RBS. The magnetization measurements suggest that more than 90% of the copper ions exist in the Cu^{2+} state in the glasses, while the XPS data show that less than 50% of the copper ions may be in the Cu^{2+} state. The low Cu^{2+} states detected by XPS may have resulted form reduction of copper ions upon exposure of the samples to X-ray radiation during measurement.

1. Introduction

Oxide glasses containing large concentrations of other transition metal ions have been studied mainly because of their semiconducting properties [1–3] and potential applications [4, 5]. The general condition for semiconducting behaviour is that the transition metal ion should be capable of existing in more than one valence state, so that the conduction can take place by the transfer of electrons from low to high valence states. Copper exists in various glasses in two oxidation states, monovalent (Cu^+) and divalent (Cu^{2+}) [6]. Each of these has different electronic structure and coordination geometry. Thus, the structures and properties of such glasses (i.e. electrical, optical, magnetic and mechanical, etc.) depend on the proportion of different valence states of copper. Hence, the ability to control and measure the ratio of Cu^{2+} and Cu^+ is important for an investigation of the effect of copper valence states on the structure and properties of these glasses. As Cu^+ ($3d^{10}$) is diamagnetic while Cu^{2+} ($3d^9$) exhibits paramagnetism, this ratio is generally examined by EPR studies [7]. In the present work we used magnetization and X-ray photoelectron spectroscopy (XPS) studies to determine the $[Cu^{2+}/Cu_{total}]$ ratio in copper phosphate glasses.

It appears from the literature that little attention has been paid to compositional changes in going from batch to glass. When phosphate glass is prepared, phosphates which are not connected with cations (copper) react with moisture in the air to produce phosphoric acid during melting. This acid easily vaporizes and fumes at higher temperature [8] and for this reason the composition of the glass may be different from that of the batch which may influence the $[Cu^{2+}/Cu_{total}]$ ratio in the glass. Hence in the present work the relative atomic concentrations of phosphorus, copper and oxygen were determined using Rutherford backscattering spectrometry (RBS). The number of Cu^{2+} will be obtained from the magnetization data giving the $[Cu^{2+}/Cu_{total}]$ ratio present in the copper phosphate glasses for each batch composition. These results are compared with the X-ray photoelectron spectroscopy (XPS) study performed on the same samples.

2. Experimental procedure

The glasses were prepared by melting dry mixtures of CuO and P_2O_5 in alumina crucibles with composition $[(CuO)_x(P_2O_5)_{1-x}]$ where $x = 0.10, 0.20, 0.25, 0.30, 0.40$ and 0.50. All chemicals used in this study were of reagent grade. The oxidation and reduction reactions in a glass melt are known to depend on the size of the melt, the sample geometry, whether the melt is static or stirred, thermal history, and quenching rate. To keep these factors constant, all glass samples were prepared under the same conditions as follows. About 40 g chemicals were mixed to obtain homogenized batches. The crucible containing the batch was placed in a furnace, heated at 300 °C for 1 h prior to melting the mixture in order to minimize volatilization. The crucible was then transferred to a melting furnace

* Author to whom all correspondence should be addressed.

0022–2461

maintained at a temperature of 1330 °C. The melt was left for about 4 h under atmospheric conditions in the furnace. During this time the melt was occasionally stirred with an alumina rod. The homogenized melt was then cast on to a stainless steel plate mould. The samples were disc shaped with diameter of ~1.5 cm and thickness of about 3 mm.

The RBS was used with 2 MeV He^{2+}. The system has been described elsewhere [9]. Briefly, a solid state detector (Tennelec model PD-50-100-14-CB) was placed in the chamber at a scattering angle of 164°, with an effective solid angle of 1.75 m.s.r. The composition of the sample was measured with an accuracy greater than ± 3%, as a large beam spot (diameter > 2 mm) was used and each sample was measured at least twice. A gold film deposited on a silicon substrate was used in calibrating the channel-energy scale of the detection system. The collected RBS spectra were then fitted by the code RUMP [10] to find the relative concentrations of various elements in the sample.

The field-dependent d.c. magnetization measurements were performed by an EG and G Princeton Applied Research (PAR) Model 155 vibrating sample magnetometer (VSM) at room temperature with applied field values ranging from 0–10 kOe. The temperature-dependent measurements were also performed on the VSM using a 1 kOe field strength with the temperature being slowly swept from 7 K to room temperature. The data have been corrected for the sample holder magnetization which was measured after each sample measurement. The overall accuracy of the magnetization measurements is estimated to be approximately 5%.

The XPS measurements were carried out with a V.G. Scientific ESCALAB MKII spectrometer equipped with a dual aluminium–magnesium anodes. Details of the system are given elsewhere [11]. The energy scale of the spectrometer was calibrated using Cu $2p_{3/2}$ = 932.4 eV and the energy separation between Cu $2p_{3/2}$ and Cu $2p_{1/2}$ of 19.8 eV. The charging of non-conducting glass samples was avoided by flooding the sample with a separate source of low-energy electrons. The energy and intensity of these external electrons were adjusted to obtain the best resolution as judged by the narrowing of the full width at half maximum (FWHM) of photoelectron peaks. It was found that at the optimum settings of the neutralizing gun (electron kinetic energy between 5 and 10 eV, electron emission current at the sample between 1 and 5 nA), the position of the adventitious C 1s line was within ± 0.5 eV of 284.6 eV. This peak arises due to hydrocarbon contamination and its binding energy is generally accepted as remaining constant irrespective of the chemical state of the sample. For the sake of consistency all energies are reported with reference to the C 1s transition at 284.6 eV. For XPS measurements, the standard oxide powder samples were embedded in substrates of indium foil supported by metallic backing. The samples were loaded through a fast-entry airlock into a preparation chamber and finally into the analysis vessel. The base pressure in the analysis chamber during these measurements was less than 5×10^{-11} mbar.

3. Results and discussion

A typical RBS spectrum from a glass sample is shown in Fig. 1. Edges of the overlapping bands corresponding to the elements copper, phosphorus and oxygen are seen. The collected RBS spectra were then fitted by the code RUMP [10], to find the relative concentrations of various elements in the glass. Spectra similar to this were obtained for the other compositions. The results are given in Table I.

The results of the magnetization, M, as a function of the magnetic field, H, at room temperature are shown in Fig. 2 as plots of M versus H/T. In a magnetic field, an atom with angular momentum quantum number, J, has $2J + 1$ equally spaced energy levels. The magnetization, M, is given by

$$M = NgJ\mu_B B_J(x) \quad (1a)$$

$$x = (gJ\mu_B H/K_B T) \quad (1b)$$

where μ_B is the Bohr magneton, K_B the Boltzmann constant, $g = 2$, $J = \frac{1}{2}$ for Cu^{2+}, and $B_J(x)$ is the Brillouin function defined as

$$B_J(x) = [(2J + 1)/2J] \coth [(2J + 1)x/2J] - [(1/2J) \coth (x/2J)] \quad (1c)$$

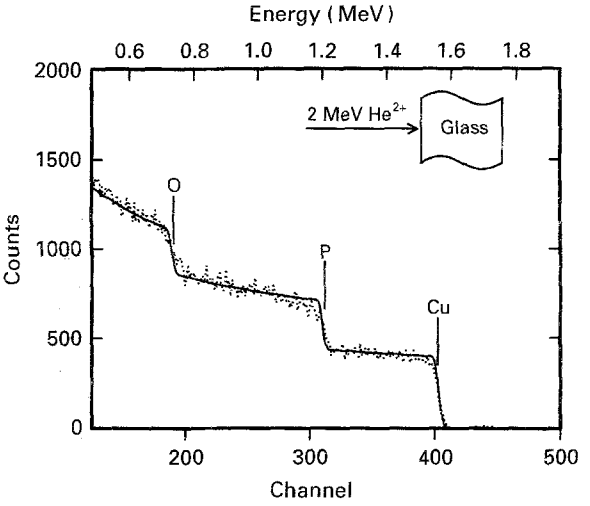

Figure 1 RBS spectrum (2 MeV $^4He^{2+}$ analysis) of a glass sample with composition $[(CuO)_{0.20}(P_2O_5)_{0.80}]$ (...) overlaid with the corresponding theoretical fit (—) as generated by the code RUMP [10].

TABLE I Relative atomic concentration of various elements in the batch as well as the glass for compositions $[(CuO)_x(P_2O_5)_{1-x}]$

x	Batch			Glass		
	Cu	P	O	Cu	P	O
0.10	0.015	0.277	0.708	0.103	0.236	0.696
0.20	0.033	0.267	0.700	0.088	0.224	0.688
0.25	0.044	0.261	0.696	0.096	0.246	0.658
0.30	0.055	0.255	0.691	0.100	0.233	0.667
0.40	0.080	0.240	0.680	0.131	0.213	0.656
0.50	0.111	0.222	0.667	0.123	0.175	0.702

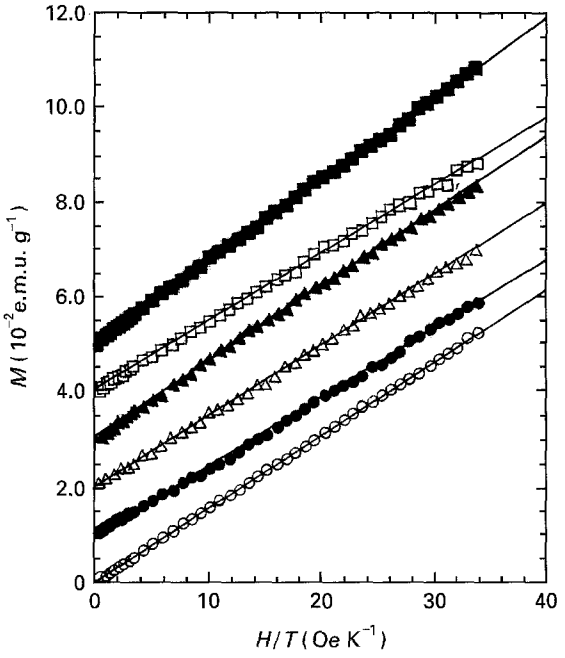

Figure 2 The field-dependent magnetization, M, for $[(CuO)_x(P_2O_5)_{1-x}]$, $x = (\bigcirc)$ 0.10, (●) 0.20, (△) 0.25, (▲) 0.30, (□) 0.40 and (■) 0.50 at room temperature as plots of M versus H/T. (●) Experimental data, (——) the fit to the data.

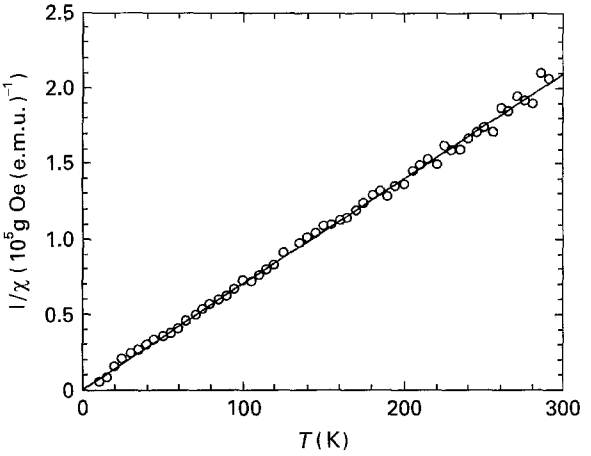

Figure 3 D.c. susceptibility of $[(CuO)_x(P_2O_5)_{1-x}]$, $X = 0.4$ as a plot of $1/\chi$ versus T. (——) The Curie–Weiss behaviour.

Recognizing that even at room temperature, Equation 1 reduces to the usual functional form of

$$M = Ng^2\mu_B^2 J(J+1)H/3\,K_BT \qquad (2)$$

The magnetization data for the glasses were fitted to Equation 2 assuming that the contribution to the magnetization was only due to Cu^{2+} ions with $J = \frac{1}{2}$. The number of Cu^{2+} ions was used as the adjustable parameter to obtain the best fit to the experimental data. An excellent agreement was obtained which is shown by the solid lines in Fig. 2. The number of Cu^{2+} ions g^{-1} samples needed to fit the data obtained for each fit is given in Table II. The d.c. magnetic susceptibility data are shown for a representative sample ($x = 0.4$) in Fig. 3 as a plot of $1/\chi$ versus T. The susceptibility follows a Curie–Weiss behaviour: $\chi = C/(T - \theta)$. For a temperature range of $\approx$ 10–300 K (the highest temperature of measurements), the susceptibility for a Curie–Weiss behaviour results in a Curie constant of 1.52×10^{-3} e.m.u. K g^{-1} and a paramagnetic Curie temperature of ≈ 0 K. Similar fitting was also applied to the $1/\chi$ versus T data. The error associated with M versus H/T data is less than 5%, while $1/\chi$ versus T data have increasing uncertainty with increasing temperature. So the number of Cu^{2+} ions g^{-1} given in Table II are those outlined from M versus H/T data. It is clear from Table II, that almost all copper exists in the Cu^{2+} state in these glasses except for $x = 0.4$, which is not understood. It is also clear from Table II, that the difference between the batch composition and glass composition is greater for lower copper concentration in the starting material which can be explained as follows. P_2O_5 contains non-bridging oxygens and thus addition of alkali or alkaline-earth oxides tend to strengthen the structure because the cations can locate between non-bridging oxygens. Phosphates which are not connected with copper react with moisture in the air to produce phosphoric acid during melting. This acid is easily fumed at high temperature. For lower concentrations more phosphates are free to make phosphoric acid resulting in a greater loss of phosphorus and hence a greater copper concentration in the glass.

Core level spectra of the Cu 2p for CuO and copper phosphate glasses of different CuO concentration, are shown in Fig. 4. The Cu 2p spectrum for the copper phosphate glasses exhibits the spin-orbit components Cu $2p_{3/2}$ and Cu $2p_{1/2}$ at binding energies of $\sim$932.5 and 952.6 eV, respectively, with satellites at about 10 eV higher binding energy. Furthermore, the 2p peaks show doublet structure (peaks marked A and B in Fig. 4). The separation between peaks A and B is

TABLE II Number of Cu_{total} ions g^{-1} in the batch as well as the glass, number of Cu^{2+} ions g^{-1} from magnetization data and Cu^{2+}/Cu_{total} ratio from magnetization and XPS for compositions $[(CuO)_x(P_2O_5)_{1-x}]$

x	Cu_{total} g^{-1} (N_A)		Cu^{2+} g^{-1} (N_A)	Cu^{2+}/Cu_{total} (%)	
	Batch composition	RBS	M versus H/T	Magnetization and RBS	XPS
0.10	0.000 74	0.004 12	0.004 08	~ 95	40
0.20	0.001 54	0.003 74	0.003 57	95	48
0.25	0.001 98	0.003 96	0.003 92	100	49
0.30	0.002 43	0.004 13	0.004 17	100	50
0.40	0.003 42	0.005 05	0.003 81	75	43
0.50	0.004 52	0.005 03	0.004 56	91	34

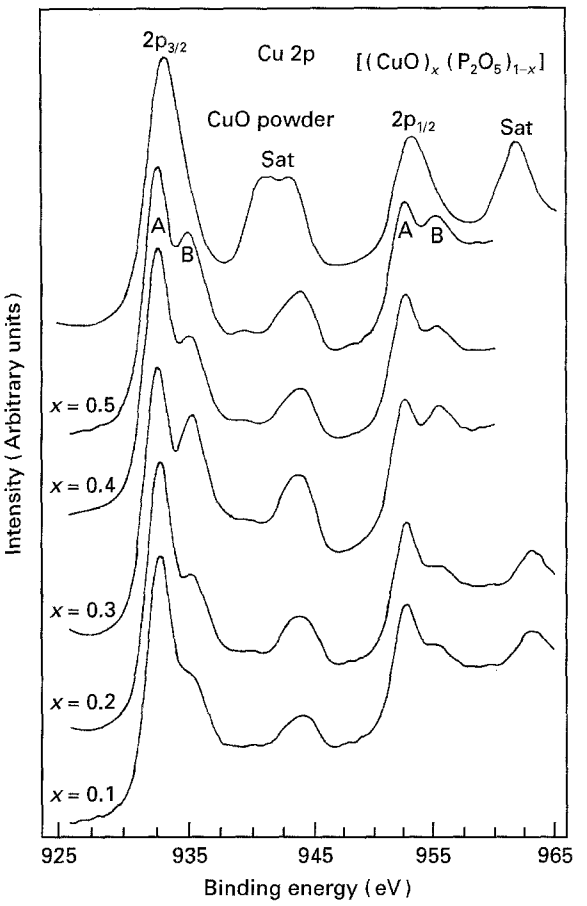

Figure 4 Core level spectra of the Cu 2p in CuO_2 powder and copper phosphate glasses.

about 2.4 eV. Monovalent and divalent are the only two oxidation states in which copper exists in various glasses [6]. Furthermore, it is well known that copper compounds containing Cu^{2+} are associated with strong satellites (this can also be seen in the present work in the CuO spectra, Fig. 4), while compounds with Cu^{+} have no satellites [12–15]. A decrease in the intensity of the satellite peak is observed upon going from CuO to copper-phosphate glass, which suggests that some of the Cu^{2+} present in the CuO are reduced to Cu^{+} in the glass. Moreover, the satellite structure (Fig. 4) clearly follows the trend of peak B, i.e. the intensity/peak height of the satellite increases with an increase in the height of peak B. Thus it may be concluded that the peaks A and B are associated with Cu^{+} and Cu^{2+}, respectively.

A deconvolution method in which the Cu 2p spectrum is assumed to be composed of two overlapping peaks was undertaken. Each component peak in the spectrum was fitted to a sum of weighted Lorentzian–Gaussian peaks with a linear sloping background by means of a least-squares fitting programme [16]. A best fit to the experimental data was found by varying the peak position, width, and intensity of each of the two component peaks. This is shown only for $x = 0.3$ in Fig. 5 and using these peaks areas, the ratio of Cu^{2+} ions was calculated as follows

$$Cu^{+} \alpha \text{ (area under peak A)} = A_A \quad (3a)$$

$$Cu^{2+} \alpha \text{ (area under peak B + area under satellite peak)} = A_B \quad (3b)$$

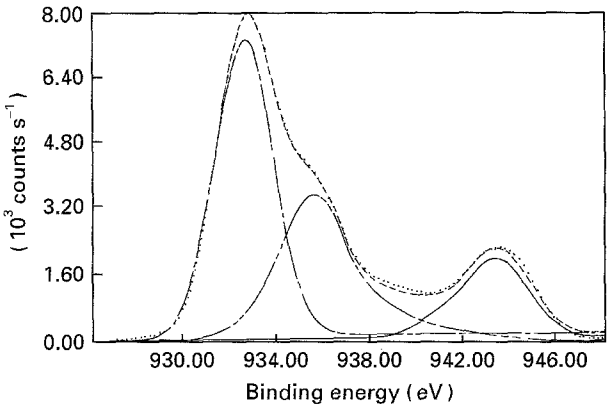

Figure 5 Cu $2p_{3/2}$ spectra for $X = 0.3$. (···) Experimental data, (— —) the fitted sum of the area of the peaks.

Then

$$Cu^{2+}/(Cu^{+} + Cu^{2+}) = A_B/(A_A + A_B) \quad (3c)$$

This ratio is shown in Table II, as a function of glass composition, x. The large difference between the findings (i.e. the ratio Cu^{2+}/Cu_{total}) of XPS and magnetization as observed from Table II may be explained as follows. XPS is just a surface study and the surface may be contaminated by exposing it even to the open atmosphere. Secondly, the oxidation states of the transition metals might be affected by the surface analytical probe as has been reported elsewhere [17]. It has been found that the transition metal ions (particularly Cu^{2+}) are susceptible to X-ray-induced reduction during XPS analyses and so on the surface the relative ratio of the ions in different valency states may not be the same as in the bulk. Similar reduction of Mo^{6+} to Mo^{5+} (or Mo^{4+}) upon irradiation with X-rays has also been observed in an XPS study of MoO_3 samples [18].

4. Conclusion

XPS, magnetization and RBS investigations were carried out on copper phosphate glasses. It was observed that compositional changes take place in going from batch to glass and these changes are copper concentration dependent, being large for low copper concentration in the batch material. Furthermore, it was observed from RBS and magnetization study that almost all copper exists in the Cu^{2+} state in these glasses, while XPS data indicated that less than 50% of the copper ions may be in the Cu^{2+} state. The large difference between the findings of XPS and magnetization may be a consequence of the reduction of copper ions when exposed to X-ray radiation.

Acknowledgements

The support of the KFUPM Physics Department, Energy Research Laboratory and Research Committee (Grant PH/PHYSPROP/43) is acknowledged.

References

1. N. F. MOTT, *J. Non-Cryst. Solids* **1** (1968) 1.
2. L. MURAWSKI, C. H. CHUNG and J.D. MACKENZIE, *ibid.* **32** (1979) 91.

3. M. SAYER and A. MANSINGH, *Phys. Rev.* **B6** (1972) 4629.
4. C. F. DRAKE, I. F. SCANLAN and A. ENGEL, *Phys. Status Solidi* **32** (1969) 193.
5. G. R. MORIDI and C. A. HOGARTH, *Int. J. Electron* **44** (1978) 297.
6. C. R. BAMFORD, "Colour generation and control in glass" (Elsevier Scientific, Amsterdam, 1977).
7. E. BAIOCCHI, A. MONTENERO, and M. BETTINELLI, *J. Non-Cryst. Solids* **46** (1981) 203.
8. B. S. BAE and M. C. WEINBERG, *J. Am. Ceram. Soc.* **74** (1991) 3039.
9. E. E. KHAWAJA, F. F. AL-ADEL, A. B. HALLAK, M.M. AL-KOFAHI and M. A. SALIM, *Thin Solid Films* **192** (1990) 149.
10. L. R. DOOLITTLE, *Nucl. Instrum. Methods* **B15** (1986) 227.
11. E. E. KHAWAJA, Z. HUSSAIN, M. S. JAZZAR and O. B. DABBOUSI, *J. Non-Cryst. Solid* **93** (1987) 45.
12. G. A. VERNON, G. STUCKY and T. A. CARLSON, *Inorg. Chem.* **15** (1976) 278.
13. K. S. KIM, *J. Electron Spectrosc. Rel. Phenom.* **3** (1974) 217.
14. SVEN LARSSON and M. BRAGGA, *Chem. Phys. Lett.* **28** (1977) 596.
15. G. VAN DER LAAN, C. WESTRA, C. HAAS and G. A. SWATZKY, *Phys. Rev.* **B23** (1981) 4369.
16. A PROCTOR and P. M. A. SHERWOOD, *Anal. Chem.* **52** (1980) 2315.
17. R. K. BROW in "Characterization of ceramics," Materials Characterization Series, edited by R. E. Loehman (Butterworth-Heinemann, 1993) p. 106.
18. R. J. COLTON, A. M. GUZMAN and J. W. RABALAIS, *J. Appl. Phys.* **49** (1978) 4090.

Received 19 August 1994
and accepted 22 March 1995